

Optically active inverse opal photonic crystals

Ke Hou, Wajid Ali, Jiawei Lv, Jun Guo, Lin Shi, Bing Han, Xiaoli Wang, and Zhiyong Tang

J. Am. Chem. Soc., **Just Accepted Manuscript** • Publication Date (Web): 19 Nov 2018

Downloaded from <http://pubs.acs.org> on November 19, 2018

Just Accepted

“Just Accepted” manuscripts have been peer-reviewed and accepted for publication. They are posted online prior to technical editing, formatting for publication and author proofing. The American Chemical Society provides “Just Accepted” as a service to the research community to expedite the dissemination of scientific material as soon as possible after acceptance. “Just Accepted” manuscripts appear in full in PDF format accompanied by an HTML abstract. “Just Accepted” manuscripts have been fully peer reviewed, but should not be considered the official version of record. They are citable by the Digital Object Identifier (DOI®). “Just Accepted” is an optional service offered to authors. Therefore, the “Just Accepted” Web site may not include all articles that will be published in the journal. After a manuscript is technically edited and formatted, it will be removed from the “Just Accepted” Web site and published as an ASAP article. Note that technical editing may introduce minor changes to the manuscript text and/or graphics which could affect content, and all legal disclaimers and ethical guidelines that apply to the journal pertain. ACS cannot be held responsible for errors or consequences arising from the use of information contained in these “Just Accepted” manuscripts.



Optically active inverse opal photonic crystals

Ke Hou,^{†,‡,§,¶} Wajid Ali,^{†,‡} Jiawei Lv,[†] Jun Guo,[#] Lin Shi,[†] Bing Han,[†] Xiaoli Wang[†] and Zhiyong Tang^{*,†}

[†]CAS Key Laboratory of Nanosystem and Hierarchical Fabrication, CAS Center for Excellence in Nanoscience, National Center for Nanoscience and Technology, Beijing 100190, P. R. China

[‡]Center for Nanochemistry, Peking University, Beijing 100871, P. R. China

[§]University of Chinese Academy of Sciences, Beijing 100049, P. R. China

[#]Membrane and membrane process laboratory, CenerTech Tianjin Chemical Research and Design Institute Limited Liability Company, 300131, Tianjin, China.

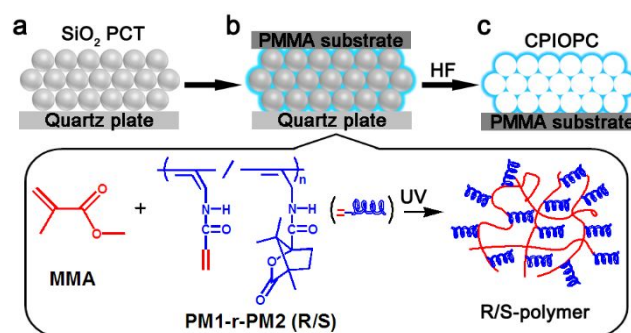
Supporting Information Placeholder

ABSTRACT: Chiral photonic crystals have been a widely investigated topic in chemistry, physics and biology. Till now, the researches about chiral photonic crystals are conducted on the objects of helical structures, while the chiral photonic crystals made of periodic chiral media remain unexplored experimentally. In this work, we have successfully constructed three-dimensional chiral polymer inverse opal photonic crystals (3D CPIOPCs) by a template-based method. Impressively, the 3D CPIOPCs exhibit emerging circular dichroism responses near the photonic band gaps. The experiments and calculations clearly elucidate the contribution of photonic structures and chiral media to this characteristic optical activity.

Chiral photonic crystals have drawn much attention in recent years due to their unique capacity in modulating the right-handed circularly polarized (RCP) and left-handed circularly polarized (LCP) lights.¹ Generally, there are two different design principles to afford the chiral photonic crystals, namely structural chirality and media chirality. The former relies on the helical arrangement of achiral building blocks, while the later bases on the intrinsic chirality of the composed materials.² To date, the research community mainly focuses on chiral photonic crystals of structural helicity. These structures are ubiquitous in nature, such as beetles³ and butterfly.⁴ Inspired by nature, scientists develop not only bottom-up self-assembly methods,⁵ but also top-down techniques⁶ to construct various helical metamaterials.⁷ However, the photonic crystals composed with chiral media are not experimentally reported yet, though theoretical works have predicted they may present many intriguing optical properties like polarization-sensitive transmission⁸ and negative refraction.⁹ Therefore, to fabricate chiral media photonic crystals and further study their optical properties are of great importance for both fundamental science and practical application.

Opal photonic crystals, which are easily achieved by the self-assembly of uniform silica or polymer nanospheres, have been extensively employed as the templates to prepare porous films

with highly-ordered inverse opal structures.¹⁰ Similarly to the templates used, these porous films possess distinct photonic band gaps (PBGs), which could be simply tuned by changing the size of nanospheres.¹¹ Herein, we utilize the silica nanospheres based photonic crystals as the templates, and infiltrate chiral polymer precursor solution to fabricate three-dimensional chiral polymer inverse opal photonic crystals (3D CPIOPCs). As-synthesized CPIOPCs exhibit the emerging circular dichroism (CD) responses near the PBGs, and R and S enantiomer CPIOPCs show the mirror-image CD signals.



Scheme 1. Protocol for preparation of CPIOPC. (a) Assembly of silica nanoparticles into PCT. (b) Infiltration of chiral polymer precursor solution into PCT. The inset displays the polymerization reaction happening inside template. (c) Construction of CPIOPC via chemical etching of silica nanoparticles by hydrofluoric acid.

To fabricate 3D CPIOPCs, monodisperse silica spheres with diameter of 174 nm, 190 nm, 195 nm, 200 nm and 210 nm, respectively, were firstly prepared by the modified Stöber methods (Figure S1).¹² Subsequently, 3D photonic crystal templates (PCTs) were formed on the quartz plates via self-assembly of silica nanoparticles by vertical deposition method (Scheme 1a, Figure S2-S4).^{10a} As expected, the PCTs display bright colors and typical PBGs (Figure S5). Afterwards, the exposed surfaces of PCTs were covered with polymethyl methacrylate (PMMA) plates (Scheme 1b). The chiral precursor solution was then infiltrated into the PCTs, in which poly(N-

propargyl acrylamide)-random-poly(N-propargyl-(R/S)-camphanamide) (PM1-r-PM2) was photo-cross-linked with methyl methacrylate (MMA) to obtain the stable chiral polymer (inset in Scheme 1b). The PM1-r-PM2 (Figure S11), which was pre-synthesized through the polymerization reaction of N-propargyl acrylamide (M1, Figure S6, S7) and N-propargyl-(R/S)-camphanamide (M2, Figure S8-S10) monomers, could be photopolymerized with other vinyl-containing monomer to get the stable and optically active polymer (Figure S12).¹³ When the polymerization reaction was finished, the silica nanoparticles in PCTs were etched in hydrofluoric acid, accompanying with peeled off from the quartz plates. Finally, the 3D CPIOPCs on the PMMA substrates (Scheme 1c) were produced.

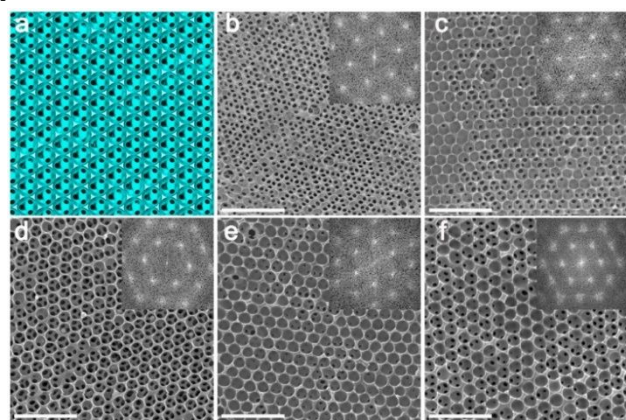


Figure 1. Structural characterization of CPIOPCs. (a) Schematic representation of (111) crystal face of CPIOPC. (b-f) Top-view SEM images of CPIOPCs fabricated from PCTs built with silica nanospheres in diameters of (b) 174 nm, (c) 190 nm, (d) 195 nm, (e) 200 nm and (f) 210 nm. Scale bars: 1 μm . The insets present the diffraction patterns obtained via fast Fourier transform of SEM images.

Figure 1a is the schematic representation of CPIOPC (111) crystal face and same with the top-view SEM images of the fabricated CPIOPCs (Figure 1b-f). The surface and cross-sectional observations (Figure S13) demonstrate the CPIOPCs successfully replicate the 3D periodic structures of PCTs, which are further evidenced by the sharp diffraction patterns (Insets in Figure 1b-f and S13). Note that by infiltrating chiral precursor solution containing PM1-r-PM2 (R) or PM1-r-PM2 (S) (Figure S10), R-CPIOPCs and S-CPIOPCs are acquired, respectively.

Diffused transmittance CD (DTCD)¹⁴ and UV-Vis absorption spectra are utilized to measure the optical property of CPIOPCs (Figure 2a-e). Evidently, the CPIOPCs show bright colors (insets) and present typical PBGs in the visible range from 400 nm to 600 nm (bottom curves in Figure 2a-e). The PBGs display small blue shift compared with those of PCTs (Table S1), which is reasonable considering the fact that the calculated effective refractive index of CPIOPCs is smaller than that of silica PCTs (Figure S14).^{11a} With respect to the optical activity of R-CPIOPCs and S-CPIOPCs (top curves in Figure 2a-e), the intense CD signals with opposite sign in the UV region from 275 nm to 425 nm originate from the infiltrated chiral polymer (Figure S15), while the new CD responses appear near the PBGs with negative sign for R-CPIOPCs and positive sign for S-CPIOPCs. Noteworthy, the CD peak position is easily tuned by changing the diameter of silica nanospheres that constitute PCTs (Figure 2f). In addition, the linear dichroism (LD) spectra of CPIOPCs

were also recorded to exclude possible LD artifact.¹⁵ As manifested in Figure S16, the contribution of the LD effect is quite weak to be negligible. Moreover, there are no obvious CD signals near the photonic band gaps when pure R- and S-polymer films are placed over top of or beneath the photonic crystals (Figure S17), demonstrating that the observed CD signals in CPIOPCs are not an artefact of the optics.

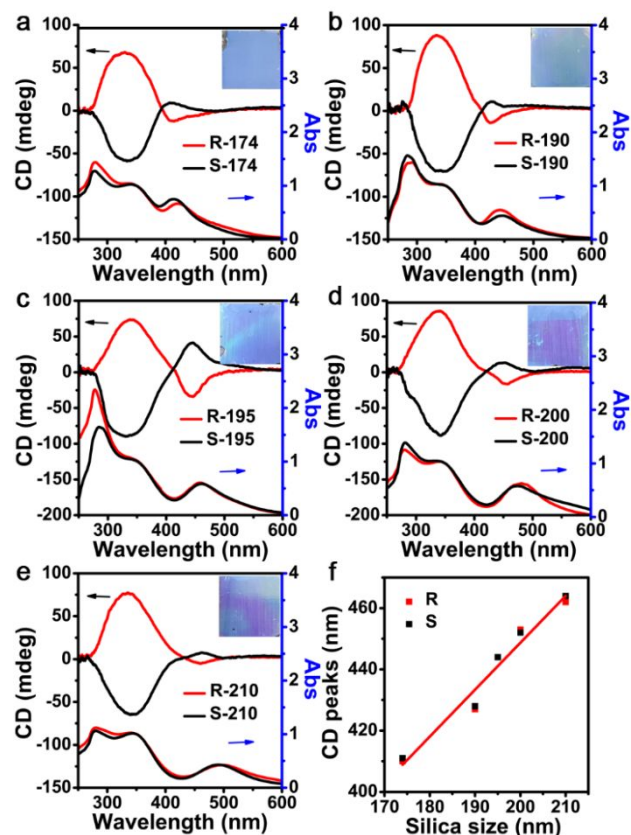


Figure 2. Optical activity of CPIOPCs. (a-e) DTCD (upper half) and UV-Vis absorption spectra (bottom half) of R-CPIOPCs and S-CPIOPCs constructed from PCTs built with silica nanospheres in diameter of (a) 174 nm, (b) 190 nm, (c) 195 nm, (d) 200 nm, (e) 210 nm. R-174 represents R-CPIOPC built with silica nanospheres of 174 nm. Insets are the typical photos of the corresponding CPIOPCs (sizes: 1 cm \times 1 cm). (f) Relationship of CD peak wavelengths of R-CPIOPCs and S-CPIOPCs with diameters of the silica nanospheres constituting the PCTs.

To verify the CD responses near the PBGs are the intrinsic optical activity of CPIOPCs, we infiltrated ethylene glycol into CPIOPCs because of its low volatility. Obviously, the CPIOPCs become transparent (insets in Figure 3a-e), and accordingly the PBGs in UV-Vis spectra totally disappear (Figure 3a-e). This is because the difference of the refractive indices between chiral polymer ($n = 1.58$, Figure S14) and ethylene glycol ($n = 1.43$) is too small. As a result, the PBGs are too weak to be detected neither by the naked eye nor through the spectroscopy machine. As expected, the CD signals of CPIOPCs near PBGs also turn to zero. This control experiment demonstrates the emerging CD responses of CPIOPCs are closely related to the PBGs. In addition, achiral PMMA inverse photonic crystals^{10a} were also constructed using the silica PCTs (Figure S18). Evidently, the CD signals for all PMMA inverse opal photonic crystals are almost zero around the PBGs (Figure 3f), disclosing the critical role of chiral media in generating the CD responses around the PBGs.

Considering the critical roles of both PBGs and chiral media, we attribute the distinct CD signals of CPIOPCs to the band gap separation in photonic crystals composed of chiral media.^{8,16} Specifically, in regard of the Bragg reflection from 3D achiral photonic crystals, the optical mode of RCP and LCP light are degenerate. Therefore, the CD signals are zero, which are consistent with the result of PMMA inverse opal photonic crystals. When the chirality is introduced, LCP and RCP lights experience the different refractive indexes in chiral media, so the PBG structures of CPIOPCs become nondegenerate state, causing non-zero CD signals near the PBGs.

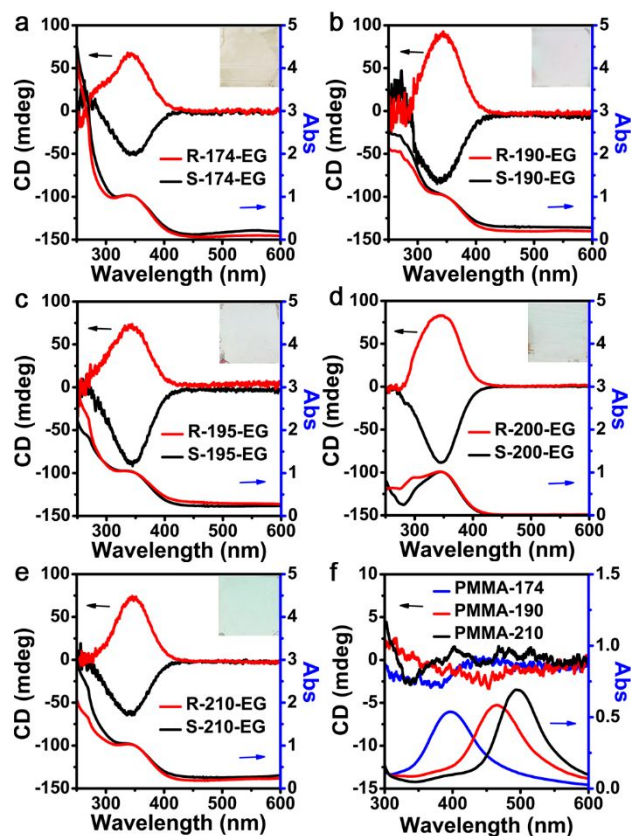


Figure 3. Optical property of control samples. (a-e) DTCD and UV-Vis absorption spectra of R-CPIOPCs and S-CPIOPCs constructed from PCTs built with silica nanospheres in diameter of (a) 174 nm, (b) 190 nm, (c) 195 nm, (d) 200 nm and (e) 210 nm after infiltration with ethylene glycol (EG). Insets are photos of the samples after infiltration with EG (sizes: 1 cm × 1 cm). (f) DTCD and UV-Vis spectra of PMMA inverse opal photonic crystals fabricated from PCTs built with silica nanospheres in diameter of 174 nm, 190 nm and 210 nm.

To further provide solid evidence for the origin of the optical activity, the CD spectra of CPIOPCs were simulated. The optical response of homogeneous chiral media is described by the following constitutive relation:⁹

$$\begin{pmatrix} \mathbf{D} \\ \mathbf{B} \end{pmatrix} = \begin{pmatrix} \epsilon_0 \epsilon & i\beta \sqrt{\mu_0 \epsilon_0} \\ -i\beta \sqrt{\mu_0 \epsilon_0} & \mu_0 \mu \end{pmatrix} \begin{pmatrix} \mathbf{E} \\ \mathbf{H} \end{pmatrix} \quad (1)$$

where \mathbf{E} is the electric field, \mathbf{B} is the magnetic field, \mathbf{H} is the electric displacement, \mathbf{D} is the magnetic induction; ϵ , μ are the permittivity and permeability, respectively; β is the chiral parameter.¹⁷ The simulation was performed with COMSOL Multiphysics using finite element method.¹⁸ As shown in Figure S19a, the CPIOPC samples are simplified into the rectangular lattice cells located on the PMMA substrate, and modelled using

Floquet periodicity along the xy direction in the whole model box.¹⁹ The incident waves are propagated directly along the z axis. In each rectangular lattice cell, the air spheres with diameter of d are embedded in the chiral host media (Figure S19b). The permittivity ϵ (real part ϵ_1 and imaginary part ϵ_2) of the infiltrated chiral polymer are obtained by fitting experimental data in Figure S14 (Figure S21a, b). The real part of chiral parameter (β_1) denotes the rotation of the polarization ellipse (Figure S20), while the imaginary part (β_2) is related to CD. β_1 and β_2 can be calculated based on the following equations, respectively (Figure S21c, d).¹⁷

$$\theta = k_0 l \beta_1 \quad (2)$$

$$\eta = k_0 l \beta_2 \quad (3)$$

Here, θ is the optical rotation angle, η is a half of ellipticity, k_0 is the wavevector in free space and l is the thickness of chiral film. It needs to be noticed that the default built-in wave equations in COMSOL Multiphysics must be modified based on the above constitutive relations for a chiral media.²⁰ To simulate the CD spectra of CPIOPCs, the absorption cross sections for the collection of rectangular cells are firstly calculated under the excitation of LCP and RCP light, respectively, and then their combination generates the CD spectra. In addition, the UV-Vis absorption cross sections of CPIOPCs excited by linear plane wave are also simulated.

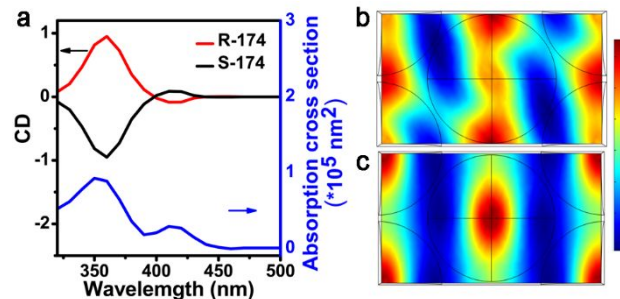


Figure 4. (a) Simulated UV-Vis absorption cross section and CD spectra of R-174 and S-174. Field distribution of (b) RCP and (c) LCP light upon the rectangular unit cell of R-174 at the band gap wavelength of 410 nm. The color represents the intensity of electric field (V/m) normal to the xy-plane.

As shown in Figure 4a, the sign and position of the simulated CD peaks, as well as the UV-Vis absorption cross section pattern, for R-CPIOPCs and S-CPIOPCs built with silica nanospheres of 174 nm in diameter (R-174 and S-174) match well with the experimental results. Figure 4b and 4c further manifest the electric field distribution of the incident LCP and RCP light upon the rectangular cells of R-174 sample at the band gap wavelength of 410 nm. Clearly, the RCP light mainly distributes on the chiral media (between air spheres) whereas the LCP wave mostly localizes in the air domain, implying the RCP and LCP modes are separated from each other. This phenomenon is reasonable because in R-CPIOPCs, the phase velocity of RCP light is smaller than that of LCP light,⁹ so the standing RCP wave concentrates in the high-index material (chiral media) while LCP wave experiences a reduced effective index (air domain).²¹ Consequently, a chiral PBG is formed. Moreover, as displayed in equation S3, with increase of the size of air spheres in the rectangular cells, the simulated PBGs and corresponding CD peaks gradually red shift (Figure S22), which are also agree well with the experimental results (Figure 2f). Altogether, the simulation reveals that the band gaps of LCP and RCP waves are separated in the inverse photonic crystals

constructed with chiral media, thus producing the CD responses at the wavelengths corresponding to the PBGs.

In summary, a simple template-based approach is developed for fabricating 3D inverse opal photonic crystals with chiral media, and their optical properties are fully investigated. As-fabricated 3D CPIOPCs display distinct CD responses near the PBGs, and R and S enantiomer CPIOPCs possess the mirror-image CD spectra. Furthermore, the CD signals at the varied wavelengths are easily acquired by selecting different sized silica nanospheres as the template materials. The theory study discloses that separation of degenerate RCP and LCP waves in chiral media is responsive for production of the CD responses near the PBGs. We believe this work will benefit not only fundamental understanding of light-matter interaction in chiral media, but also the chirality-related applications such as circularly polarizing beamsplitter,^{7b} stereoselective sensing,²⁰ asymmetrical photocatalysis, and so on.

ASSOCIATED CONTENT

Supporting Information. Additional synthesis methods, supplementary figures are available free of charge via the Internet at <http://pubs.acs.org>.

AUTHOR INFORMATION

Corresponding Author

*zytang@nanocr.cn

Author Contributions

*K.H. and W.A. contributed equally.

Notes

The authors declare no competing financial interests.

ACKNOWLEDGMENT

The authors acknowledge financial support from National Key Basic Research Program of China (2014CB931801 and 2016YFA0200700, Z.Y.T.), National Natural Science Foundation of China (21890381, 21721002 and 21475029, Z.Y.T.), Frontier Science Key Project of Chinese Academy of Sciences (QYZDJ-SSW-SLH038, Z.Y.T.), and K.C.Wong Education Foundation (Z.Y.T.).

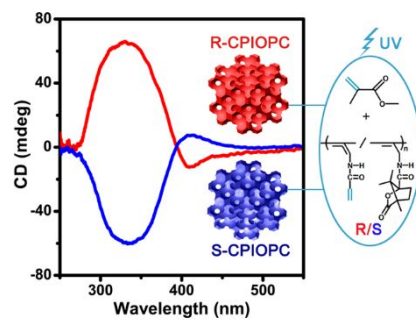
REFERENCES

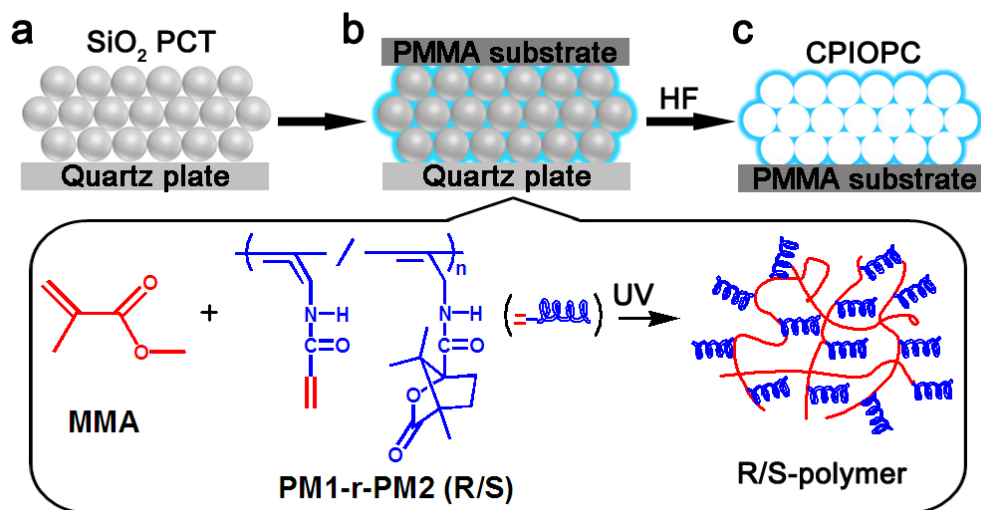
- (1) Kelly, J. A.; Giese, M.; Shopsowitz, K. E.; Hamad, W. Y.; MacLachlan, M. J. *Acc. Chem. Res.* **2014**, *47*, 1088-1096.
- (2) Li, J. Q.; Su, Q. Y.; Cao, Y. S. *Opt. Lett.* **2010**, *35*, 2720-2722.
- (3) Sharma, V.; Crne, M.; Park, J. O.; Srinivasarao, M. *Science* **2009**, *325*, 449-451.
- (4) Saranathan, V.; Osuji, C. O.; Mochrie, S. G.; Noh, H.; Narayanan, S.; Sandy, A.; Dufresne, E. R.; Prum, R. O. *Proc. Natl. Acad. Sci. U. S. A.* **2010**, *107*, 11676-11681.
- (5) (a) Wang, L.; Dong, H.; Li, Y.; Xue, C.; Sun, L.-D.; Yan, C.-H.; Li, Q. J. *Am. Chem. Soc.* **2014**, *136*, 4480-4483; (b) Shopsowitz, K. E.; Hamad, W. Y.; MacLachlan, M. J. *J. Am. Chem. Soc.* **2012**, *134*, 867-870.
- (6) (a) Thiel, M.; Decker, M.; Deubel, M.; Wegener, M.; Linden, S.; von Freymann, G. *Adv. Mater.* **2007**, *19*, 207-210; (b) Toader, O.; John, S. *Science* **2001**, *292*, 1133-1135.
- (7) (a) Gansel, J. K.; Thiel, M.; Rill, M. S.; Decker, M.; Bade, K.; Saile, V.; von Freymann, G.; Linden, S.; Wegener, M. *Science* **2009**, *325*, 1513-1515; (b) Turner, M. D.; Saba, M.; Zhang, Q.; Cumming, B. P.; Schroder-Turk, G. E.; Gu, M. *Nat. Photonics* **2013**, *7*, 801-805.
- (8) He, C.; Lu, M. H.; Yin, R. C.; Fan, T. A.; Chena, Y. F. *J. Appl. Phys.* **2010**, *108*, 2486-2491.
- (9) Christofi, A.; Stefanou, N. *J. Opt. Soc. Am. B* **2012**, *29*, 1165-1171.
- (10) (a) Hu, X.; An, Q.; Li, G.; Tao, S.; Liu, J. *Angew. Chem. Int. Ed.* **2006**, *45*, 8145-8148; (b) Burgess, I. B.; Mishchenko, L.; Hatton, B. D.; Kolle, M.; Lončar, M.; Aizenberg, J. *J. Am. Chem. Soc.* **2011**, *133*, 12430-12432.
- (11) (a) Ge, J.; Yin, Y. *Angew. Chem. Int. Ed.* **2011**, *50*, 1492-1522; (b) Huang, Y.; Zhou, J.; Su, B.; Shi, L.; Wang, J.; Chen, S.; Wang, L.; Zi, J.; Song, Y.; Jiang, L. *J. Am. Chem. Soc.* **2012**, *134*, 17053-17058.
- (12) Stöber, W.; Fink, A.; Bohn, E. *J. Colloid Interface Sci.* **1968**, *26*, 62-69.
- (13) Du, X.; Liu, J.; Deng, J.; Yang, W. *Polym. Chem.* **2010**, *1*, 1030-1038.
- (14) Górecki, M. *Chirality* **2015**, *27*, 441-448.
- (15) (a) Cao, Y.; Che, S. *Chem. Mater.* **2015**, *27*, 7844-7851; (b) Rong, Y.; Chen, P.; Liu, M. *Chem. Commun.* **2013**, *49*, 10498-10500.
- (16) Li, J. Q.; Jin, L.; Li, L.; Li, C. F. *IEEE Photonics Technol. Lett.* **2006**, *18*, 1261-1263.
- (17) Oh, S. S.; Hess, O. *Nano Convergence* **2015**, *2*, 24-34.
- (18) Lei, Q.-L.; Ni, R.; Ma, Y.-q. *ACS Nano* **2018**, *12*, 6860-6870.
- (19) Salski, B. *Prog. Electromagn. Res. M* **2012**, *27*, 27-39.
- (20) Nesterov, M. L.; Yin, X.; Schäferling, M.; Giessen, H.; Weiss, T. *ACS Photonics* **2016**, *3*, 578-583.
- (21) von Freymann, G.; Kitaev, V.; Lotsch, B. V.; Ozin, G. A. *Chem. Soc. Rev.* **2013**, *42*, 2528-2554.

1
2
3
4
5
6
7
8
9
10
11
12
13
14
15
16
17
18
19
20
21
22
23
24
25
26
27
28
29
30
31
32
33
34
35
36
37
38
39
40
41
42
43
44
45
46
47
48
49
50
51
52
53
54
55
56
57
58
59
60

Insert Table of Contents artwork here

Table of Contents (TOC)





Scheme 1. Protocol for preparation of CPIOPC. (a) Assembly of silica nanoparticles into PCT (b) Infiltration of chiral polymer precursor solution into PCT. The inset displays the polymerization reaction happening inside template. (c) Construction of CPIOPC via chemical etching of silica nanoparticles by hydrofluoric acid.

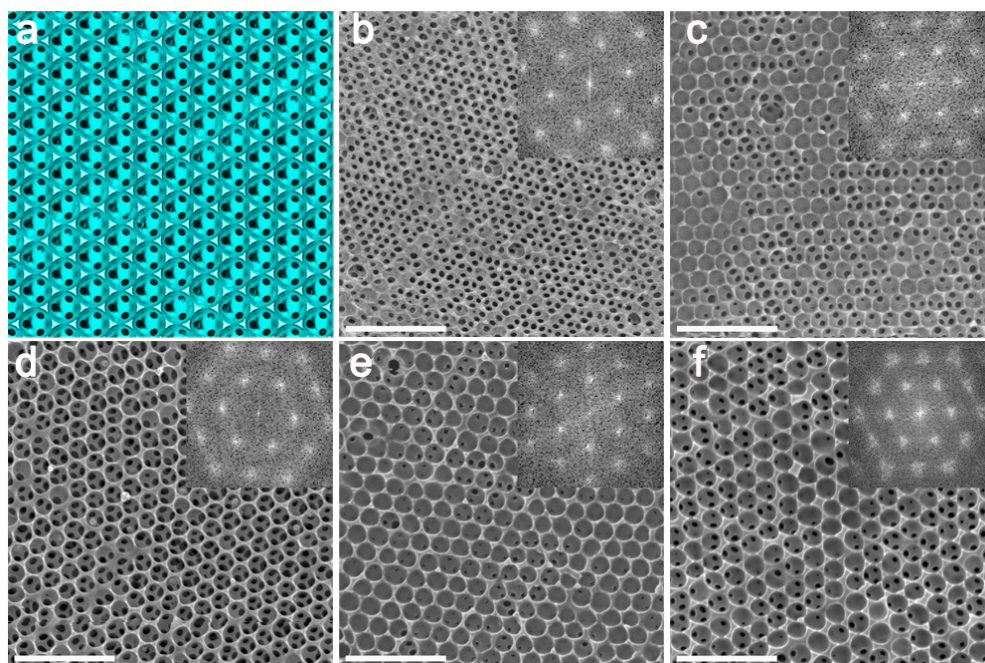


Figure 1. Structural characterization of CPIOPCs. (a) Schematic representation of (111) crystal face of CPIOPC. (b-f) Top-view SEM images of CPIOPCs fabricated from PCTs built with silica nanospheres in diameters of (b) 174 nm, (c) 190 nm, (d) 195 nm, (e) 200 nm and (f) 210 nm. Scale bars: 1 μm . The insets present the diffraction patterns obtained via fast Fourier transform of SEM images.

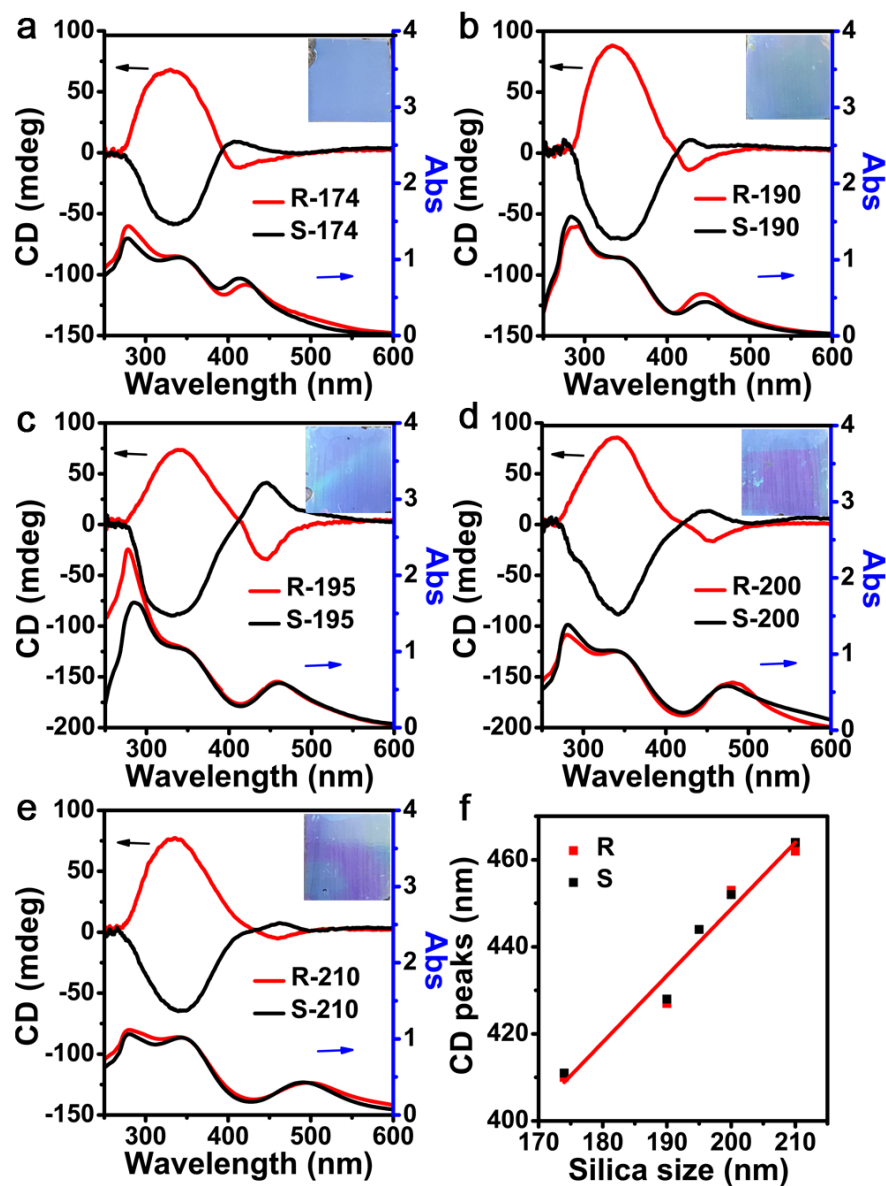


Figure 2. Optical activity of CPIOPCs. (a-e) DTCD (upper half) and UV-Vis absorption spectra (bottom half) of R-CPIOPCs and S-CPIOPCs constructed from PCTs built with silica nanospheres in diameter of (a) 174 nm, (b) 190 nm, (c) 195 nm, (d) 200 nm, (e) 210 nm. R-174 represents R-CPIOPC built with silica nanospheres of 174 nm. Insets are the typical photos of the corresponding CPIOPCs (sizes: 1 cm \times 1 cm). (f) Relationship of CD peak wavelengths of R-CPIOPCs and S-CPIOPCs with diameters of the silica nanospheres constituting the PCTs.

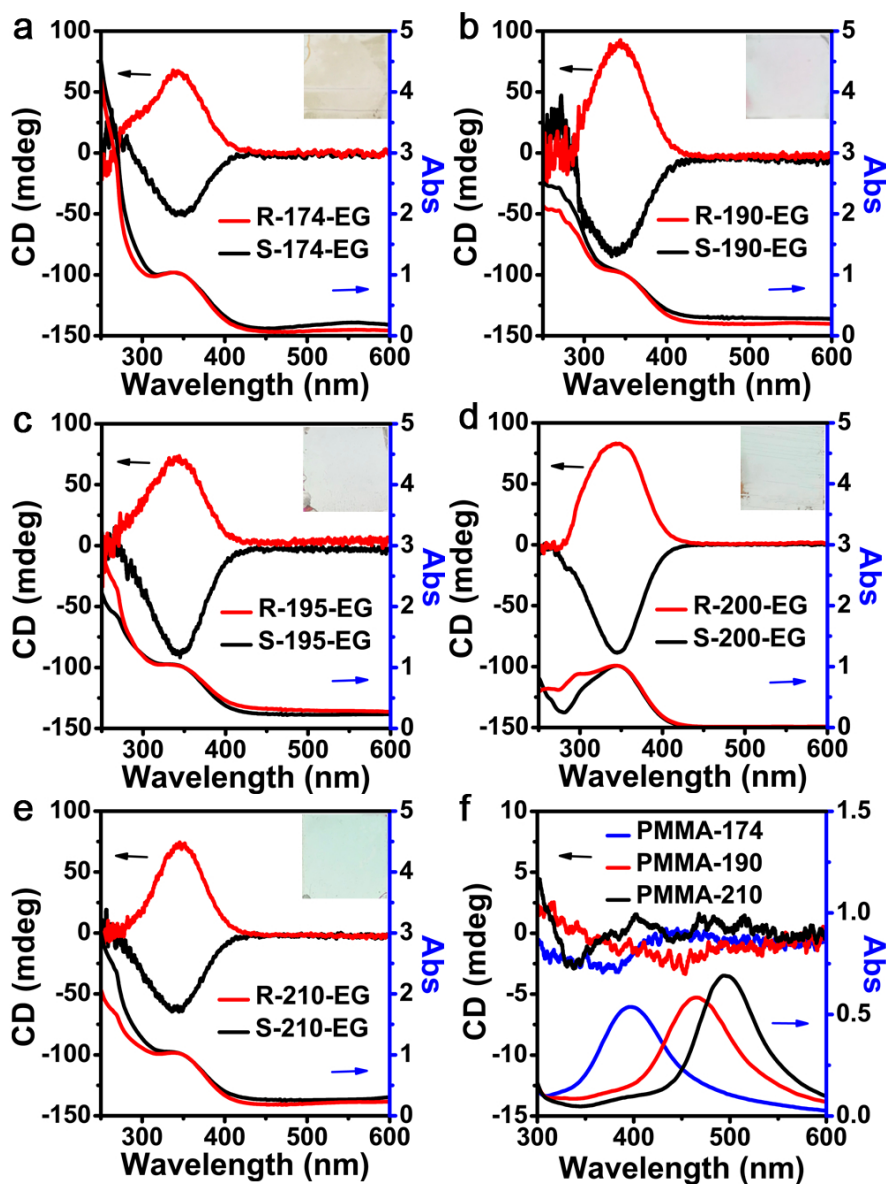


Figure 3. Optical property of control samples. (a-e) DTCD and UV-Vis absorption spectra of R-CPIOPCs and S-CPIOPCs constructed from PCTs built with silica nanospheres in diameter of (a) 174 nm, (b) 190 nm, (c) 195 nm, (d) 200 nm and (e) 210 nm after infiltration with ethylene glycol (EG). Insets are photos of the samples after infiltration with EG (sizes: 1 cm \times 1 cm). (f) DTCD and UV-Vis spectra of PMMA inverse opal photonic crystals fabricated from PCTs built with silica nanospheres in diameter of 174 nm, 190 nm and 210 nm.

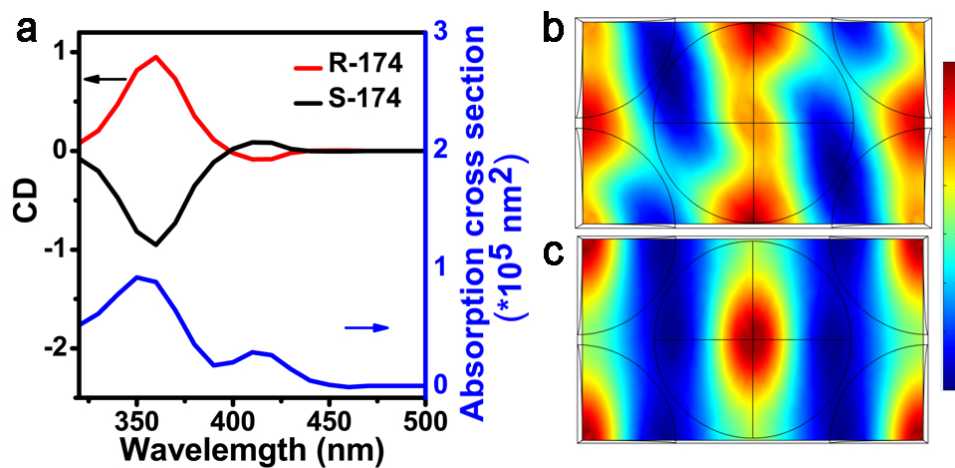


Figure 4. (a) Simulated UV-Vis absorption cross section and CD spectra of R-174 and S-174. Field distribution of (b) RCP and (c) LCP light upon the rectangular unit cell of R-174 at the band gap wavelength of 410 nm. The color represents the intensity of electric field (V/m) normal to the xy-plane.

